
High Energy Diffuse Gamma-Rays from Galactic Plane

Nobuhito TATEYAMA

Institute of Physics, Kanagawa University, Yokohama 221-8686, Japan

Jun NISHIMURA

Institute of Space and Aeronautical Science, Sagamihara 229-8510, Japan

Abstract

The dominant part of the diffuse gamma rays beyond 1 TeV from the Galactic plane has been thought as due to the inverse Compton scattering of interstellar photons with high-energy cosmic-ray electrons. In these energy regions, diffuse gamma-ray observations give us unique information on the energy spectrum of high-energy electron in the interstellar space, since we cannot observe those electrons directly. We made a calculation with $|b| \leq 2^\circ$ and $|b| \leq 5^\circ$ for the diffuse gamma rays in the case of 3 spatial distribution in the Galaxy of cosmic-ray sources, and the results are compared with the most recent observed data by air shower experiments. We draw a restriction for the injection spectrum of high-energy electrons at the sources. It is also pointed out that patchy structure of the gamma-ray distribution will appear at high-energy side, if we observe the distribution with a higher angular resolution of a few arc degrees. This patchy structure will become distinct beyond 10 TeV of IC gamma rays, where number of contributing sources of parent electrons decrease and their diffusion distance become smaller.

1. Formulations

We calculate the electron spectrum by using a diffusion model. Ignoring the effect of the radial diffusion, electron flux J_e at a distance, z , perpendicular to the Galactic plane after they accelerated t years ago, is given by,

$$J_e(E, z, t) = Q(E) \frac{(1 - bEt)^{\gamma-2}}{\sqrt{4\pi D1}} \exp\left(\frac{-z^2}{\sqrt{4\pi D1}}\right)$$

$$D1 = D_0(E/GeV)^\delta (1 - bEt)^{1-\delta} / (1 - \delta)bE,$$

where b is the coefficient of energy loss by synchrotron and inverse Compton processes. Q is the production spectrum at the source, and assumed to be a

Table 1. Injection spectral index of the electrons at the source and diffusion coefficient. $1/b=2.3 \times 10^5 \text{ yr.TeV}, < B^2 >^{1/2}$ is assumed to be $6.7 \mu\text{G}$ (Webber²⁰)

Index γ	2.4	2.2	2.0
δ	0.3	0.5	0.5
$D_0(\text{cm}^2/\text{s})$	4×10^{28}	10^{28}	10^{28}

power spectrum of $E^{-\gamma}$. In Table 1, numerical parameters used in this work are listed. If we take the thickness of the source distribution as $z_0 \sim 100 \text{ pc}$, the electron spectrum is written by a power law with a special index of $-\gamma - (1 + \delta)/2$ (Ginzburg et al.⁷) around $10 \text{ GeV} \sim 100 \text{ TeV}$. The absolute value of the electron flux was fixed to agree with the observed data at 10 GeV (Nishimura et al.¹⁶). For radial distribution of electron sources in the Galactic plane, we assume uniform, Gaussian distribution with $\sigma=10 \text{ kpc}$ (Bloemen et al.³) and Kodaira's SNR Distribution. The interstellar radiation field (ISRF) components must be considered to the inverse Compton process as for the cosmic background radiation (CMB). From the observations (IRAS, COSB/DIRBE and the radio observations), the emission contributing to ISRF can be divided into stellar and dust emission depending on their wavelength. The stellar emission contains UV, optical and near-infrared in the wavelength range up to $8 \mu\text{m}$, and are assumed to be a mixture of four-components given by Mathis et al.¹³ and Bloemen³. The dust emission in the wavelength range from 8 to $1000 \mu\text{m}$ has a peak at around $100 \mu\text{m}$ and $10 \mu\text{m}$. This surface brightness can be decomposed into five-components given by Cox et al.⁶. For total energy density of the ISRF, we adopt the results estimated by Strong et al.¹⁹ for both stellar and dust components. In the high-energy region above 100 TeV , absorption of the gamma rays by the collision with the CMB is taken into account in the calculation (Gould and Schreder⁸). The gamma-ray energy spectrum $J_\gamma(\epsilon, l, b)d\epsilon$ is given by

$$J_\gamma(\epsilon, l, b)d\epsilon = d\epsilon \int \int \int \phi(R, l) \psi(R, z) \Lambda(kT, \epsilon) J_\epsilon(E, z, t) \frac{d^2 N_{\gamma, \epsilon}}{dt dE} dt dl dE$$

$$R^2 = L \cos^2 b + R_s^2 - 2LR_s \cos b \cos l$$

, where $d^2 N_{\gamma, \epsilon}/dt dE$ is the gamma-ray production rate by the inverse Compton process of Klein-Nishina cross section (Blumenthal and Gould⁴). $\phi(R, l)$ is the radial distribution of electron, $\psi(R, z)$ is the spatial energy density distribution of the ISRF and $\Lambda(kT, \epsilon)$ is the absorption probability of gamma rays. R_s is the distance from the Sun to the Galactic center, R is the distance measured

from the Galactic center to a point in the plane, L is the line-of-sight distance. We assume that R_s is 8.5 kpc and the radius of the Galaxy is 15 kpc.

2. Energy Spectrum

Figure 1 shows the diffuse gamma-ray energy spectrum due to the inverse Compton scattering in the direction $l = b = 0^\circ$. Here we also plotted each contribution due to the CMB, the radiation of stellar and dust emission. The radial distribution of electron is the Gaussian distribution with σ of 10kpc. The figure shows that the contribution due to the stellar emission is dominant to the gamma rays below 0.1 TeV, and the dust emission is not negligible compare to that due to the CMB around 10 TeV. The gamma-ray spectrum of our result is higher than that given by Porter and Protheroe (for the case of no cut-off energy of the primary acceleration). The reason of this difference mainly due to the energy dependence of diffusion coefficient of E^δ . In our calculation, we take $\delta = 0.3$ and $D_0 = 4 \times 10^{28}[\text{cm}^2/\text{s}]$ at 1 GeV, Porter and Protheroe takes $\delta = 0.6$ and $D_0 = 2.5 \times 10^{28}[\text{cm}^2/\text{s}]$ at 3 GeV. The electron flux in our calculation is about a factor 2 higher compared to Porter's at 50 TeV, which is mainly contributing for gamma rays around 10 TeV. Above 200 TeV, the absorption process due to photon-photon collisions with CMB becomes important. The energy spectra from the Galactic plane, averaged over the latitude range $|b| \leq 1^\circ$, $|b| \leq 5^\circ$ and $|b| \leq 10^\circ$ for Gaussian radial distribution, are shown in Figure 2. We can precisely determine the injection index with good angular resolutions of $|b| \leq 1^\circ$ or $|b| \leq 2^\circ$. According to the work of Hunter et al., flux of gamma rays due to π^0 for $|b| \leq 10^\circ$ are almost the same flux of the inverse Compton process at 0.1 TeV. Figure 3,4 show the gamma-ray energy spectrum of $|b| \leq 2^\circ$ and $|b| \leq 5^\circ$ for Gaussian distribution with the most recent results of the Tibet experiment (Amenomori et al.²) and other results by the Whipple (LeBohec, S et al.¹³), the HEGRA (Ahronian, F.A. et al.¹), and the CASA-MIA (Borione et al.⁵). The experimental data show upper limit of the gamma-ray flux. We can exclude the hard spectral index, smaller than 2.0 of the injection spectral index of electron at the source.

3. Patchy Structure of Gamma-ray Distribution

The diffuse gamma rays here calculated are the average feature of the gamma-ray flux. However, very high-energy electrons are not distributed continuously in the Galactic plane assuming their sources are SNR. The electrons of 50TeV contribute to gamma rays of energy around 10TeV by the inverse Compton scattering with CMB. The lifetime of the 50TeV electrons is about 4×10^3 yrs by the energy loss of synchrotron and inverse Compton processes. Assuming that

the supernova accelerates those electrons and the burst rate of super nova is 1/30 yrs in the Galaxy, we expect almost 100 active sources in the Galaxy contributing to 50 TeV electrons. The diffusion distance of those electrons is expected as $(2DT)^{1/2} \sim 150$ pc. Therefore, electrons of 50 TeV are localized near the sources, and are clumped in almost 100 small spots distributed in the Galactic plane (Figure 5,6). The inverse Compton gamma rays are produced from these local spots. The average angular separation of those spots seen from the solar systems are a few degrees, but we would observe some bright nearby sources with larger separation. In fact, we already observed some bright high-energy gamma-ray point sources such as SN1006 and Crab nebula. Thus, the granule structure of diffuse gamma rays is to be observed for gamma rays beyond about 10TeV, if we observe with a certain angular resolution. This patchy structure would become clear at higher energy region. Thus, at high energy region, we can observe continuous diffuse gamma rays due to π^0 produced by protons added by the IC gamma rays of point source like structure.

4. Discussions and Conclusions

In our calculation, we take the parameters of injection spectra of the electrons and the diffusion coefficient to agree with the experimental data of the direct electron observations. The gamma-ray spectrum of our result is similar to that given by Porter and Protheroe (for the case of no cut off of the electron energy in the acceleration) under the different value of δ .

1. The diffuse gamma rays above 1 TeV are mainly due to the inverse Compton scattering with the CMB and the infrared radiation. The diffuse gamma rays produced by the inverse Compton process with stellar emission is dominant up to 0.1 TeV. The dust component also shows important contribution up to 10 TeV as the contribution of the CMB.
2. The spectral index of electrons at the source with smaller than 2.0 is excluded by the comparison to the results of the experiments (Fig.3, Fig.4).
3. There are no evidence that the anisotropy of the cosmic rays in this energy region is larger than 10^{-3} in 100 TeV region. It seems that the index δ is not so large compare to 0.5 in the case of $\gamma = 2.2, 2.0$.
4. As the energy of parent electrons increase, electrons cannot diffuse far away and are confined near the source. Since the lifetime of those electrons decrease with energy, the number of contributing sources also decrease with energy. Those sources are to be observed as the point source like distribution with minor diffusive parts of gamma rays beyond 10 TeV.

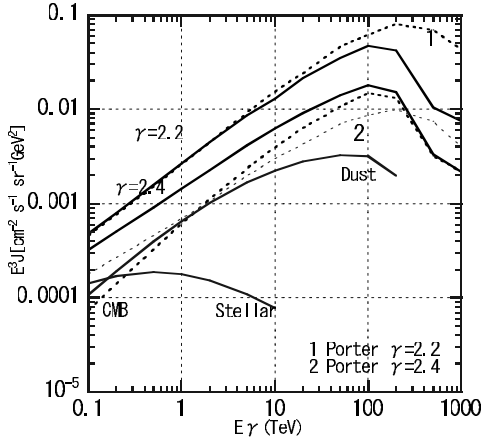


Fig.1 The diffuse gamma-ray energy spectra with $\gamma = 2.2, 2.4$, in the direction $l = b = 0^\circ$. The solid line shows total intensity due to the CMB, stellar, and dust components. The broken lines (1, 2) show the result by Porter et al. with $\gamma = 2.2, 2.4, \delta = 0.6$ (no cut-off of the electron energy in the acceleration).

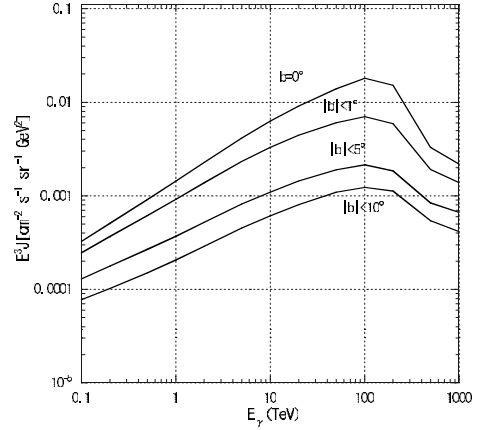


Fig.2 The energy spectra, averaged over the latitude range $|b| \leq 1^\circ, |b| \leq 5^\circ$ and $|b| \leq 10^\circ$ with $\gamma = 2.4$ in the direction $l = b = 0^\circ$. The solid line shows $l = b = 0^\circ$. The energy spectrum contains all gamma rays due to the CMB, stellar, and dust components.

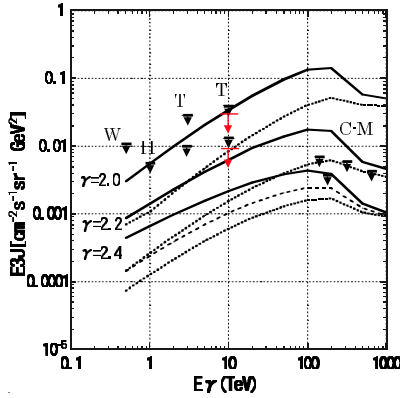


Fig.3 The diffuse gamma-ray energy spectra for $|b| \leq 2^\circ$. The solid line shows the spectra in the direction $l = 0^\circ$, the dotted line shows the spectra in the direction $l = 180^\circ$. The broken line shows the spectra in the direction $l = 90^\circ$ ($\gamma = 2.4$).

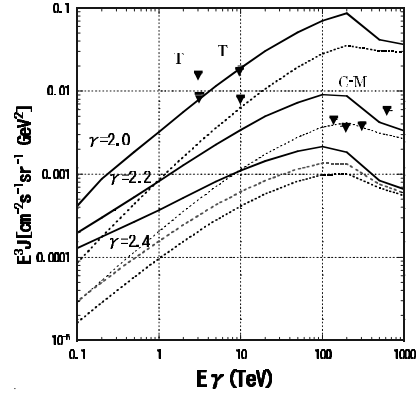


Fig.4 The diffuse gamma-ray energy spectra for $|b| \leq 5^\circ$. The solid line shows the spectra in the direction $l = 0^\circ$, the dot-line shows that in the direction $l = 180^\circ$. The broken-line shows that in the direction $l = 90^\circ$ ($\gamma = 2.4$).

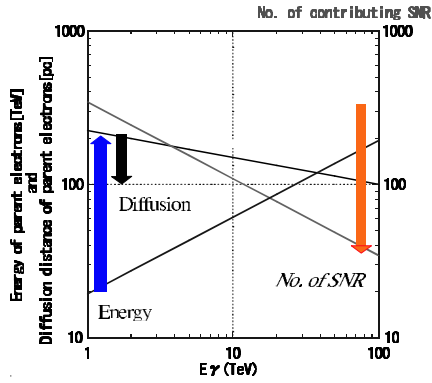


Fig.5 Energy of parent electrons, diffusion distance of parent electron and number of SNR. E_γ is averaged energy of inverse Compton process, $\delta=0.3$, D_0 is $4 \times 10^{28} \text{cm}^2/\text{s}$ at 1 GeV, lifetime of electrons by synchrotron is 2×10^8 yrs at 1 GeV, and burst rate of SNR is 1/30 yrs.

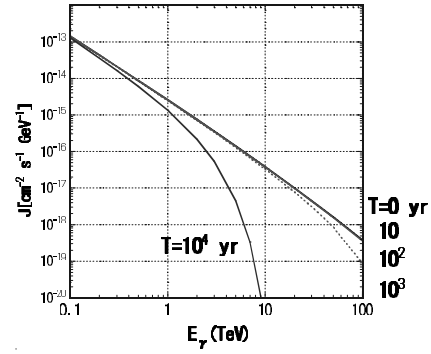


Fig.6 Inverse Compton energy spectra from the point source after T years from their production with $\gamma=2.4$. The total energy Q_0 greater than 1 GeV is 10^{48} erg. The distance from the Solar system is 1.7 kpc.

5. References

1. Aharonian, F.A. 2001, *A&A*, 375, 1008
2. Amenomori, et al. 2002, *ApJ*, 580
3. Bloemem, J.B.G.M., et al. 1993, *Astron. Astrophys.*, 267, 372
4. Blumenthal, G.R. and Gould, R.J. 1970, *Rev. Mod. Phys.*, 42, 237
5. Borione, A et al. 1988, *ApJ*, 493, 175
6. Cox, P., et al. 1986, *Astron. Astrophys.*, 155, 380
7. Ginzburg, V.L. 1990, *Astrophysics of Cosmic rays*, North Holland
8. Gould, R.J and G.P. Schreder, G.P. 1967, *Phys. Rev.*, 155, 1404
9. Hunter, S.D., et al. 1997, *ApJ*, 481, 205
10. Karle, A. et al. 1995, *Phys. Letts*, B347, 161
11. Kobayashi, K., et al. 1999, *Proc. 26th ICRC*, 3, 61
12. LeBohec, S., et al. 2000, *ApJ*, 539, 209
13. Mathis, J.S., Mezger, P.G., Panagia, N. 1983, *Astron. Astrophys.*, 128, 212
14. Mori, M. 1997, *ApJ*, 478, 225
15. Nishimura, J., et al. 1980, *ApJ*, 238, 394
16. Porter, T.A., Prothro, R.J. 1997, *J. Phys.* G23, 1765
17. Reynolds, P.T., et al. 1993, *ApJ*, 404, 206
18. Strong, A.W., Morskalko, I.V., Reimer, O. 2000, *ApJ*, 537, 763
19. Torii, S., et al. 2001, *ApJ*, 559, 973
20. Webber, W.R., et al. 1980, *ApJ*, 236, 448